Journal of Manufacturing Innovations
2024, VOL. 1, NO. 3, 1–7
DOI: 10.22055/jomi.2024.47002.1020

Failure analysis of austenitic stainless steel AISI 304 Exhaust bag filter at Sanati Dodefam Co.

Fatemeh Alijani[1], Mohammad Jula[1]*, Mohammad Narimani[1], Sajad Vahabi[1], Hossein Assadollah Zadeh[2], Payam Pooryazdi[2], Hassan ShalBaf[2], Ali Amir Gholami[2]

[1]KADFA Company, Ahvaz, Iran
[2]Sanati Dodefam Company, Dezful, Iran

ABSTRACT

In the current investigation, experts from Kavoshgaran Danesho Fan Apadana (KADFA) examined the root causes of sever corrosion in the exhaust bag filter fabricated from AISI 304 stainless steel at Sanati Dodefam Co., located in Khuzestan Province. Various structural analyses and microstructural examinations were conducted for this purpose. The results of chemical composition determination of the corrosion products using EDS and XRF indicated a significant presence of sulfur and chlorine, further confirmed by XRD analysis. The cracks observed in the equipment body were determined to have been caused by stress corrosion cracking (SCC) based on their morphology. The formation of cracks in the weld metal was attributed to the combined effects of SCC and intergranular corrosion resulting from chromium carbide precipitation due to sensitization. The comprehensive analyses revealed that the inlet gas contained water vapor along with impurities, leading to gradual extensive uniform and localized corrosion over time.

ARTICLE HISTORY
Received 25 May 2024
Revised 28 September 2024
Accepted 5 October 2024

KEYWORDS
Corrosion
SCC
AISI 304
Structural analysis
Microstructure
Failure

1. Introduction

Field inspections uncovered severe corrosion on the body of the exhaust bag filter (Fig. 1), with characterized by significant thickness reduction and multiple cracks. Corrosion was particularly pronounced in the welded regions. Analysis of the Process Flow Diagram (PFD) provided by the company indicated that the inlet gas consisted of hydrocarbons and water vapor at a temperature of approximately 240 °C. Armed with this data, various hypotheses were formulated to guide the design of the tests and analyses, aimed at pinpointing the cause of the failure.

In the industry, Carbon Black is produced through the controlled conditions of incomplete combustion or thermal decomposition of gaseous or liquid hydrocarbons. This process involves the breakdown of hydrocarbon chains through hydrogen loss, leading to the formation of smaller radicals that eventually form carbon particles [1]. The production process occurs in harsh environmental conditions, including various corrosive compounds such as sulfur and chloride [2], which can lead to significant corrosion and mechanical failures in industrial equipment. This necessitates frequent maintenance and can result in unexpected downtime [3].

Austenitic stainless steel AISI 304 is extensively utilized in various industrial sectors, including the oil, gas, and petrochemical industries [4], due to its exceptional corrosion resistance and mechanical properties. This alloy is particularly noteworthy for its passive nature and minimal uniform corrosion rate [5]. However, under specific conditions, it can fail due to a combination of factors such as mechanical stress, high temperatures, and corrosive environments. The primary causes of failure are attributed to stress corrosion cracking (SCC) [6] and pitting corrosion [7] . The presence of aggressive substances like chlorides and acids in the production environment

* Corresponding author.
E-mail address: Mohammad.jula@gmail.com (M. Jula)

significantly contributes to corrosion and subsequent failure [7]. Chloride ions disrupt the passive film on the surface, leading to the formation of pits. High mechanical stress, especially when combined with corrosive environments, results in SCC [6] and fatigue [8], potentially causing sudden and catastrophic failure [9]. In the literature, intergranular cracks often observed by SEM caused by the precipitation of chromium carbides at grain boundaries, which depletes the chromium content in these areas and weakens the passive film [9]. While ISI 304 is generally resistant to uniform corrosion, it can still occur in highly acidic or basic environments. Although the overall rate of corrosion is usually lower compared to localized forms, it can still lead to noticeable material loss over time [10].

Despite the corrosion-resistance nature of the alloy, the AISI 304 stainless steel experienced failure at Sanati Dodefam Co. under the specified conditions. This project aimed to investigate the underlying reasons for the severe corrosion and cracking through the application of various analytical techniques.



Fig. 1. Failed exhaust bag filter with severe corrosion.

2. Materials and Methods

Multiple samples were cut from different parts of the exhaust bag filter body, and prepared for further analyses through cutting and machining. The corrosion products were mechanically removed for subsequent examination. The chemical composition of the corrosion products and the potential presence of corrosion-inducing elements were assessed using X-Ray Fluorescence (XRF). For this purpose, the samples were dried at 110 ºC and then exposed to 950 ºC to measure Loss on Ignition (L.O.I), resulting in the elements being reported in their oxidation states.

Structural analysis was conducted using X-ray diffraction (XRD) within the range of 10-90 degrees, employing a copper source (CuKα (λ=0.154 nm). Microstructural examinations were performed by an optical microscope (OM) and a scanning electron microscope (SEM) equipped with energy dispersive X-ray spectroscopy (EDS) analysis. Prior to these examinations, the cross-sections of the specimens were mounted and then ground by sandpapers ranging from 60 to 5000 grit. Polishing was performed with alumina suspension containing abrasive particles measuring 1-3 micrometers.

3. Results and Discussion

Results

Corrosion products

The XRF results for the corrosion products are detailed in Table 1. The predominant compound was identified as iron oxide (Fe_2O_3), along with sulfur compounds and other oxides. Notably, the L.O.I value in the table reflects the carbon content released as carbon dioxide when heated up to 950 °C, surpassing the carbon oxidation temperature.

Table 1. Chemical composition of the corrosion products with L.O.I.

Oxide	Fe_2O_3	SO_3	SiO_2	MgO	Cr_2O_3	Na_2O	Cl	L.O.I.
Wt.%	86.65	1.90	0.41	0.56	0.15	1.23	0.50	8.6

Table 2. Chemical composition of the corrosion products without L.O.I.

Oxide	Fe_2O_3	SO_3	SiO_2	MgO	Cr_2O_3	Na_2O	Cl
Wt.%	94.78	2.34	0.44	0.61	0.16	1.33	0.34

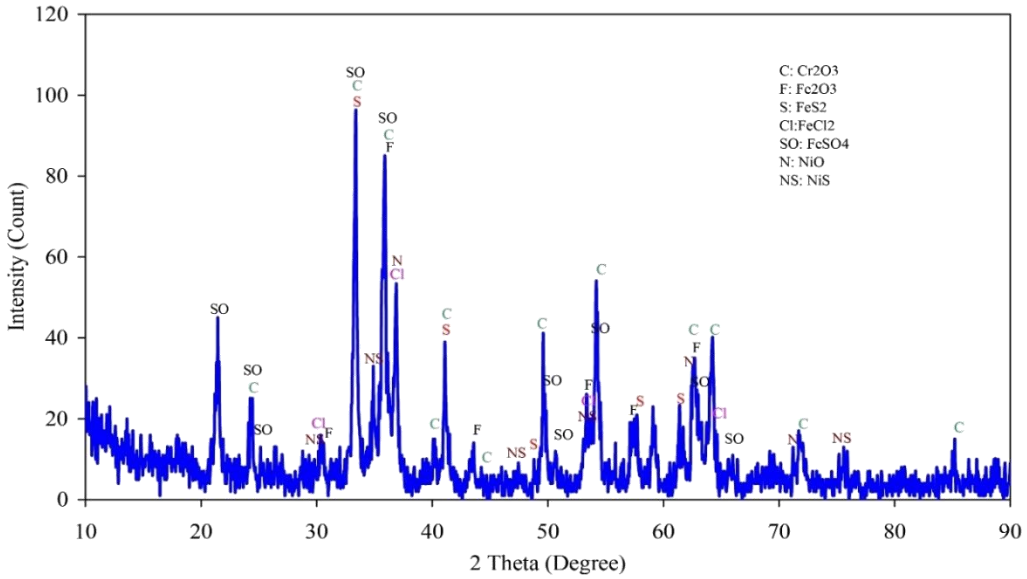


Fig. 2. XRD pattern of the corrosion products.

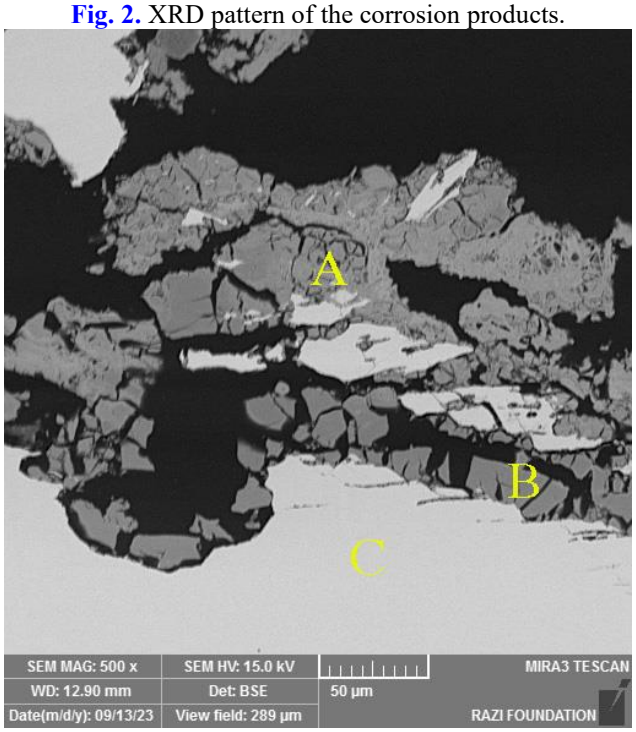


Fig. 3. SEM image of the sample cross section and corrosion products.

Table 3. Elemental analyses for corresponding points in Fig. 3.

Element	Wt.%		
	Point A	Point B	Point C
O	38.34	42.47	0.55
Si	0.69	0.62	-
S	3.30	4.50	-
Cr	31.05	47.05	18.42
Fe	23.56	1.01	72.88
Ni	3.06	4.35	8.16

Given the significant carbon content and high L.O.I in the final product, a refined XRF analysis excluding the volatile compounds was conducted to better identify minor constituents. Table 2 illustrates the noticeable presence of sulfur and chlorine.

The XRD pattern of the corrosion products, depicted in Fig. 2, reveals Fe_2O_3 as the major component, with Cr_2O_3 and other oxides as minor constituents. The detection of chromium oxide suggests the detachment of the protective oxide layer from the stainless steel due to corrosion. Consistent with the XRF findings, peaks corresponding to sulfur and chloride compounds are evident in the XRD pattern.

Owing to the localized nature of SEM images, multiple samples were examined, with the summarized results as follows. Elemental analysis (EDS) of the sample's cross section, illustrated in Fig. 3 and Table 3, indicated the presence of iron and chromium oxides (based on the percentages of oxygen, chromium, and iron) at point B in Fig.3. The chemical composition at point A closely matched that of the AISI 304 stainless steel.

In the MAP analysis shown in Fig. 4, the presence of oxygen and sulfur corroborates the findings from previous tests.

Evidence of uniform and localized corrosion

The micrographs of the samples shown in Fig. 5 revealed that both uniform and localized corrosion occurred simultaneously on the equipment body. A continuous layer of corrosion products, along with several pits, are observable in the figure.

Microstructure of the body

Fig. 6 shows the OM and SEM images of the equipment body. it is evident that cracks propagated from the corroded surface into the depths of the specimen, extending almost directly with multiple fine and coarse branches. These types of cracks are associated with SCC in the literature [11]. Apart from the crack initiation on the surface, a significant percentage originated from corrosion-induced pits (Fig, 6, (b)), indicating that the pits served as stress concentration areas.

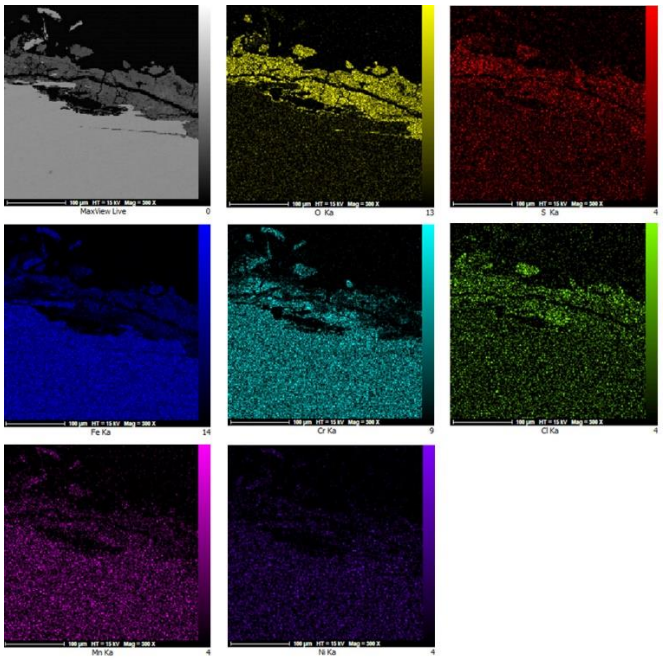


Fig. 4. MAP analysis of corrosion products.

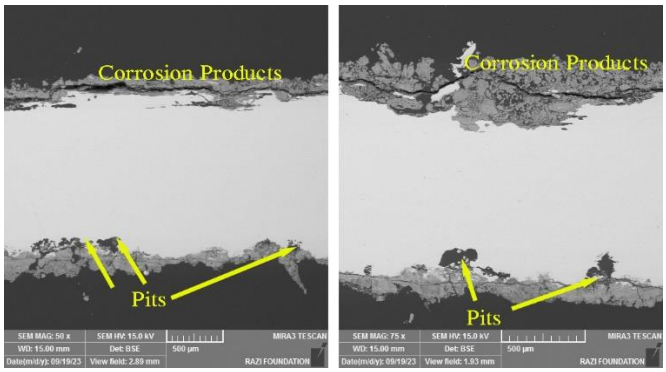


Fig. 5. SEM images of the specimens showing the continuous layers of corrosion products alongside the pits.

Welded regions

Examination of the images obtained from the OM in the welded regions (Fig. 7) revealed two major types of cracks. There are direct cracks with multiple branches (known as transgranular, Fig. 7 (a) and (b)), as well as cracks changing directions along the paths (intergranular, Fig. 7 (c)). These

cracks are the indication of susceptibility to SCC due to improper welding conditions.

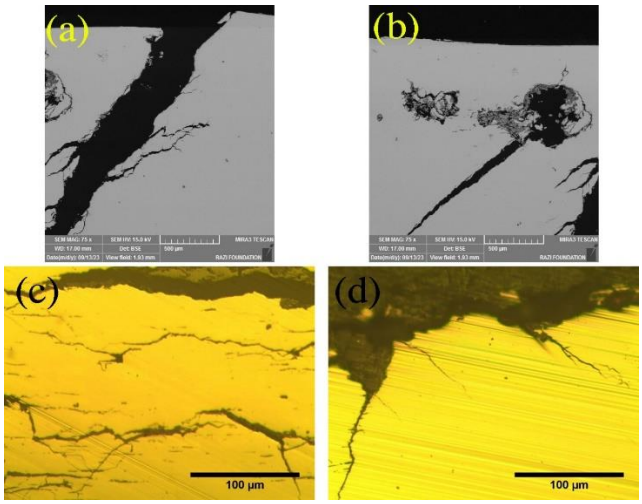


Fig. 6. (a) SEM image of the cracks initiated from the surface, (b) SEM image of the cracks initiated from a pit, (c) and (d) OM images of the cracks.

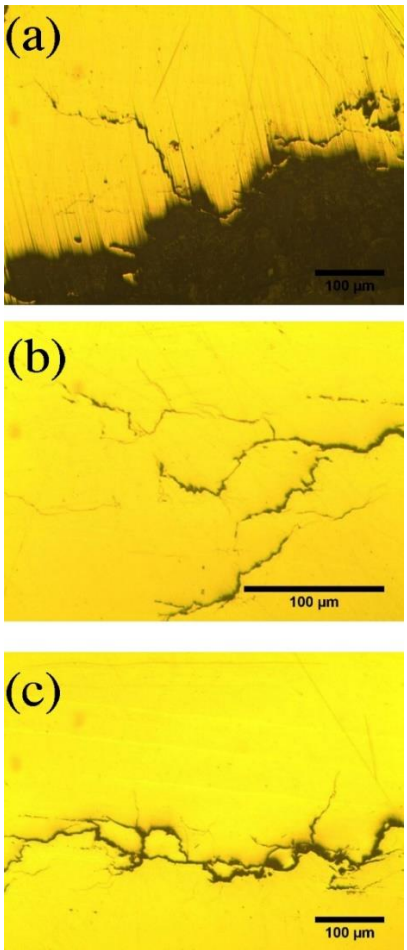


Fig. 7. OM images of the cracks formed in welded regions.

Elemental MAP analysis of the welded area (in Fig. 8) shows the presence of sulfur alongside iron/chromium oxides in the corrosion products.

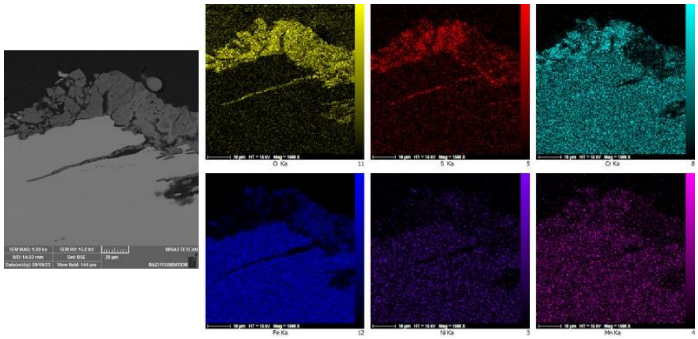


Fig. 8. Microstructure and elemental analysis of welded regions.

Discussion

Corrosion

AISI 304 stainless steel has limited usability at low acid concentrations (<5%) [12,13], particularly with sulfuric acid up to 1 M [14,15]. In the studied equipment, the temperature reportedly reached up to 240 °C. Additionally, the presence of corrosive elements, i.e., S and Cl was confirmed.

The simultaneous presence of sulfur and water in the environment surrounded AISI 304 can lead to the formation of sulfate ions (SO_4^{2-}) that penetrate the passive Cr_2O_3 layer, causing its degradation. Consequently, the breakdown of the passive layer occurs more rapidly than the process of repassivation [14,15]:

$$Fe + H_2O \rightarrow FeO + 2H^+ + 2e$$
$$Ni + H_2O \rightarrow NiO + 2H^+ + 2e$$
$$Cr + H_2O \rightarrow CrO + 2H^+ + 2e$$

While austenitic stainless steels are generally suitable for environments containing hydrogen chloride gas, the presence of moisture significantly alters their behavior. Hydrochloric acid, which is soluble in water at any concentration, dissociates into ions and attacks metal surfaces [16]. In the studied alloy, the release of hydrogen contributed to the breakdown of the protective layer. The anodic reaction within the pits involves the iron dissolution [16]:

$$Fe \leftrightarrow Fe^{2+} + 2e^-$$

Electrons migrate to the cathode (passivated surface) through the following reaction:

$$^1/_2\ O_2 + H_2O + 2e^- \leftrightarrow 2\ (OH^-)$$

As a result, positive charges outside the pits attract chloride ions:

$$FeCl_2 + 2H_2O \leftrightarrow Fe(OH)_2 + 2HCl$$

SCC

Based on the morphology of the existing cracks and considering the residual stress and the welding process, SCC occurred in the studied equipment. According to the definition provided by NACE [17], SCC refers to cracks created by corrosion and applied or residual stress in the presence of water and corrosive agents such as chlorine and amines. The level of stress required for SCC can be lower than the yield stress. In this type of cracking, failure occurs transgranularly rather than intergranularly. Common grades of stainless steels (304, 304L, 316, 316L, 321, 347, 303, 302, and 301) with an Ni content of 7-10% are prone to SCC [11,18]. However, ferritic and duplex stainless steels with an Ni content exceeding 18% exhibit enhanced resistance to SCC. Crevices, pits, wet/dry areas such as interfaces serve as initiation sites for SCC. This phenomenon can occur within a few weeks, one to two years, or even up to 10 years after exposure [18,19].

Intergranular corrosion

The morphology of the cracks formed in welded regions (Fig. 7) demonstrates cracks propagation along grain boundaries, indicating evidence of intergranular corrosion. When austenitic stainless steels are exposed to temperatures within the range of 427–899 °C, chromium along grain boundaries tends to combine with carbon to form carbides. This phenomenon, known as sensitization or carbide precipitation, reduces chromium content and decreases resistance to corrosion in areas surrounding grain boundaries. The occurrence of this process depends on both temperature and time [20].

Carbide precipitation is attributed to slow cooling rates from annealing temperature, stress relief in the sensitization temperature range, and welding. Shorter holding times during welding result in a sensitized heat-affected zone (HAZ). This type of corrosion is sensitive to the size of the exposed area and the surrounding environment. Many environments do not cause intergranular corrosion in stainless steels except acidic ones containing oxidizing agents such as sulfur and nitrogen [21].

4. Conclusions

Field inspections, as well as structural and microstructural examinations of the samples taken from the body and welded regions of the AISI 304 exhaust bag filter, revealed the extensive uniform corrosion, pitting corrosion, SCC, and intergranular corrosion. The following results highlight the susceptibility of AISI 304 stainless steel to these types of corrosion:

- XRF and XRD tests on the corrosion products confirmed the presence of S and Cl, in addition to iron/ chromium oxides.

- Multiple microstructural analyses of the corrosion products also showed sulfur- and chlorine- containing compounds. Numerous visible pits on the surface provided evidence of extensive localized corrosion.

- The microstructural images of the cracks revealed that:

- Cracks initiated from the surface and penetrated inward.

- Localized corrosion pits contributed to stress concentration sites for crack initiation.

- Multiple fine and coarse branches in the cracks, directly propagating within the material, are associated with SCC.

- The microstructural analyses of the welded regions showed:

- Direct cracks with multiple branches, indicative of SCC.

- Changed paths of the cracks due to intergranular corrosion.

Based on the obtained evidence, the primary cause of degradation in the AISI 304 stainless steel exhaust bag filter is attributed to uniform and localized corrosion in the presence of oxidizing agents and impurities in the inlet gas. The water vapor in the system likely led to the formation of condensates containing acidic compounds within the equipment, arising extensive corrosion.

Acknowledgements

The project was done by experts and researchers in KADFA Co. at the request of Sanati Dodefam Co.. All financial support provided by Sanati Dodefam Co. is much appreciated.

References

[1] I. Drogin, Carbon Black, J. Air Pollut. Control

Assoc. 18 (1968) 216–228. https://doi.org/10.1080/00022470.1968.10469118.

[2] the U.S. Environmental Protection Agency (EPA), Carbon black, (2020). https://www.epa.gov/sites/default/files/2020-10/documents/c06s01.pdf.

[3] grand view research, Carbon Black market size, 2024. https://www.grandviewresearch.com/industry-analysis/carbon-black-market.

[4] J.C.M. Farrar, The Alloy Tree, Woodhead, 2004.

[5] M.F. McGuire, Stainless Steels for Design Engineers, ASM International, 2008. https://doi.org/10.31399/asm.tb.ssde.9781627082860.

[6] S. Moore, R. Burrows, D. Kumar, M.B. Kloucek, A.D. Warren, P.E.J. Flewitt, L. Picco, O.D. Payton, T.L. Martin, Observation of stress corrosion cracking using real-time in situ high-speed atomic force microscopy and correlative techniques, Npj Mater. Degrad. 5 (2021) 3. https://doi.org/10.1038/s41529-020-00149-y.

[7] C. Lu, X. Shen, X. Cheng, C. Du, H. Ma, Corrosion Failure Analysis of 304 and 2205 Stainless Steels in High-Temperature Condensate Containing Chloride Ions, J. Mater. Eng. Perform. (2023). https://doi.org/10.1007/s11665-023-08949-4.

[8] Z. Chen, W. Lu, Y. Chen, C. Lu, Fatigue Crack Detection in AISI 304 Austenitic Stainless Steel Using Nonlinear and Linear Ultrasonic Testing Methods, J. Mater. Eng. Perform. 29 (2020). https://doi.org/10.1007/s11665-020-04914-7.

[9] S. Ahmed, Influence of high temperature on corrosion behavior of 304 stainless steel in chloride solutions, AIP Adv. 6 (2016) 115301. https://doi.org/10.1063/1.4967204.

[10] V. Shtefan, N. Kanunnikova, A. Pilipenko, H. Pancheva, Corrosion Behavior of AISI 304 Steel in Acid Solutions, Mater. Today Proc. 6 (2019) 150–157. https://doi.org/10.1016/j.matpr.2018.10.088.

[11] S.D. Cramer, B.S. Covino, eds., Corrosion: Environments and Industries, ASM International, 2006. https://doi.org/10.31399/asm.hb.v13c.9781627081849.

[12] S.M. Elsariti, Haftirman, Behaviour of Stress Corrosion Cracking of Austenitic Stainless Steels in Sodium Chloride Solutions, Procedia Eng. 53 (2013) 650–654. https://doi.org/10.1016/j.proeng.2013.02.084.

[13] P.R. RHODES, Mechanism of Chloride Stress Corrosion Cracking of Austenitic Stainless Steels, Corrosion 25 (1969) 462–472. https://doi.org/10.5006/0010-9312-25.11.462.

[14] NACE, NACE SP0204-2008, Stress Corrosion Cracking (SCC) Direct Assessment Methodology, (2008).

[15] R. M. G. D. A.-Q. George V. Chilingar, The Fundamentals of Corrosion and Scaling for Petroleum & Environmental Engineers, Elsevier, 2008. https://doi.org/10.1016/C2013-0-15528-6.

[16] H.S. Khatak and Baldev Raj, Corrosion of Austenitic Stainless Steels, Woodhead, 2002.

[17] M.A. Kappes, Localized corrosion and stress corrosion cracking of stainless steels in halides other than chlorides solutions: a review, Corros. Rev. 38 (2020) 1–24. https://doi.org/10.1515/corrrev-2019-0061.

[18] S.D. Cramer, B.S. Covino, eds., Corrosion: Fundamentals, Testing, and Protection, ASM International, 2003. https://doi.org/10.31399/asm.hb.v13a.9781627081825.

[19] k. sotoodeh, Case Studies of Material Corrosion Prevention for Oil and Gas Valves, Elsevier, 2022. https://doi.org/10.1016/C2021-0-03539-2.

[20] M. Abdallah, Corrosion behaviour of 304 stainless steel in sulphuric acid solutions and its inhibition by some substituted pyrazolones, Mater. Chem. Phys. 82 (2003) 786–792. https://doi.org/10.1016/S0254-0584(03)00367-5.

[21] M. Javidi, S.M.S. Haghshenas, M.H. Shariat, CO2 corrosion behavior of sensitized 304 and 316 austenitic stainless steels in 3.5 wt.% NaCl solution and presence of H2S, Corros. Sci. 163 (2020) 108230. https://doi.org/10.1016/j.corsci.2019.108230.